phys. stat. sol. (b) **243**, No. z, zzz–zzz (2006) / **DOI** 10.1002/pssb.200600000

# Hydride electronics

**Smagul Zh. Karazhanov*[1,2], P. Ravindran[1], P. Vajeeston[1], and Alexander G. Ulyashin[3]**

[1] *Center for Materials Sciences and Nanotechnology, Department of Chemistry, University of Oslo, PO Box 1033 Blindern, N-0315 Oslo, Norway*
[2] *Physical-Technical Institute, 2B Mavlyanov St., 700084 Tashkent, Uzbekistan*
[3] *Institute for Energy Technology, P.O.Box 40, NO-2027 Kjeller, Norway*

Received zzz, revised zzz, accepted zzz
Published online zzz

**PACS** 71.15.Mb, 71.20.-b, 71.55.-i, 78.20.-e, 81.05.-t

*Corresponding author: e-mail:smag@uzsci.net

With the help of first-principles density functional calculations, using $AlH_3$ as a model system, we have shown that some of the hydrides possess the features of transparent conducting oxides (TCO). Based on this observation we discuss here the possible novel applications of hydrides in electronic device technology as electrical conducting materials, which can have both n- and p- type conductivity and at the same time transparent in the infrared (IR), near IR, or visible regions. Moreover, some advantages concerning properties of interfaces in case of using hydrides in modern multilayer based device structures are discussed.

copyright line will be provided by the publisher

## 1 Introduction

From the mid-1990s studies on hydrides became very popular owing to their applications in “energy storage” [1, 2], switchable mirrors [2-4], rechargeable batteries [1] etc. Hydrides have also found application in composite semiconductor/electrolyte photoelectrochemical system consisting of AlGaAs, Si, and metal hydride/NiOOH, which generates a potential of 1.2–1.3 V with the efficiency of 18.1% [5], and is insensitive to variation of light intensity, i.e. the cell generates electricity not only under illumination, but also in the dark. First heterojunction based on metal $PdH_x$, proton conductor KOH, and KOH•H2O has been constructed [6], which is important for design of novel type of electrochemical devices. Recently it has been found that molecule/cluster of $Al_4H_6$ is stable with band gap of 1.9 eV between the highest occupied and lowest unoccupied molecular orbitals [7]. If one prepares $Al_4H_6$ in bulk, it will be useful not only for energy storage, but also for electronic applications.

Kinetics of hydrogen absorption/desorption processes of some hydrides are found to be fast at ambient temperatures and pressures with additives [1-3]. Although it is important for hydrogen economy, it can cause instability in electrical properties of hydrides. This may be one of the reasons why electrical properties and potential of the hydrides for applications in electronic device technology was not discussed in the scientific literature. However, nowadays some hydrides are found with slower hydrogenation/dehydrogenation kinetics at elevated temperatures. Especially complex hydrides can be stable even at high temperatures like other inorganic compounds such as oxides. These findings have led us to the idea that hydrides can be useful in electronic device technology. In this paper we explore this idea by calculations within the density-functional theory (DFT). Using $AlH_3$ as example, we have shown that

WILEY InterScience® DISCOVER SOMETHING GREAT

copyright line will be provided by the publisher

000000 physica (b) 243/z WordXP Art.: W0000/Autor M:\Brage-publikasjoner\Physica-status-solidi-A-Applied-research-.200723171.doc
&R310; insgesamt 11 Seiten 15.09.2017 Bearb.:

1 hydrides can find applications such as transparent conducting (TC) materials, buffer layer between TCOs
2 and semiconductors, novel class of spintronic materials etc.
3

4 ## 2 Computational details

5 Our study is based on DFT using the projected-augmented-wave method implemented into the VASP-
6 PAW package [4, 5]. We have used the generalized-gradient approximation with the exchange-
7 correlation functional of Perdew-Wang [6]. The self-consistent calculations were performed using a
8 $10\times10\times10$ mesh of special **k**-points. The lattice was fully relaxed using the conjugate gradient method.
9 The plane-wave cutoff energy of 500 eV was used for all the calculations which is found to be sufficient
10 to reproduce ground state and high pressure structural properties. The convergence was achieved when
11 the forces acting on the atoms were smaller than 10 meV $Å^{-1}$ and the total energy difference between two
12 consecutive iterations were < $10^{-6}$ eV. The convergence criteria and more details about the optical calcu-
13 lations were discussed in Ref. [7].
14

15 ## 3 Choice of the materials

16 We have considered hexagonal (*h*) and orthorhombic (*o*) modifications of $AlH_3$. Our choice is based
17 on the wide band gap of $AlH_3$–*h* $E_g$=3.5 eV [8] found by DFT calculations within GW approximation,
18 which is almost the same as that of the well known TCOs such as ZnO and $In_2O_3$. Furthermore, nature of
19 its chemical bonding is mixed ionic and covalent [9] character. So, well dispersive top-most valence
20 band (VB) is expected, required for good electrical conductivity.
21 $AlH_3$ is reported to form a stable crystalline solid at room temperature [10]. From *ab initio* calcula-
22 tions [11] it is found that band gap of $AlH_3$ slightly decreases with increasing the pressure. Experimental
23 studies of thermal stability show that α- and β- phases of $AlH_3$ exhibit dehydriding reactions in the tem-
24 perature range of 60-200 ºC [12], 330 ºC [13] etc., which is well above the operable range of optoelec-
25 tronic devices. Hydrogen decomposition kinetics has been found to be enhanced by doping, particle size
26 [14], and vacancy concentration [14, 15]. However, according to Ref. [16] one can store $AlH_3$-*h* for sev-
27 eral years without any loss of H. Here we use $AlH_3$-*h* and -*o* as a model system only, to demonstrate that
28 hydrides have TC and semiconducting features required for device applications, thus leaving the problem
29 of finding a more suitable hydride is open and to be the subject for the future studies.
30

31 ## 4 Results and discussion

32 Band structure for $AlH_3$-*h* and –*o* is presented in Figure 1. We shall start analysis from $AlH_3$-*h*. The
33 calculated fundamental band gap is 2.14 eV. Because of the well-known deficiency of DFT, the real gap
34 is expected to be larger than the calculated one. Consequently, these hydrides are transparent to visible
35 spectra. The calculated energy difference between the bottom-most conduction band (CB) and next near-
36 est CB minimum is $E_g^*$=1.76 eV (to be called hereafter as second band gap), which is smaller than the
37 required value $E_g^*$=3.1 eV to provide transparency in the visible spectra upon heavy n-type doping.
38 Analysis of Figure 1 shows that the bottom-most CB of $AlH_3$-*h* is well dispersive. It indicates that
39 CB electrons are able to contribute well to electrical conductivity. Our calculations show that the CB
40 electron effective masses are equal to $0.27m_0$ along $\Gamma\rightarrow F$, $Z$ and $0.32m_0$ along $\Gamma\rightarrow L$. The calculated
41 masses are in between those for the well known TCOs such as ZnO and $In_2O_3$ (experimental values are
42 $0.22m_0$ and $0.30m_0$ for ZnO and $In_2O_3$ and our corresponding calculated values are $0.147m_0$ and $0.23m_0$,
43 respectively). Consequently, $AlH_3$-*h* is expected to posses increased electron mobility upon doping with
44 shallow donors resulting good electrical conductivity.
45 Although $AlH_3$-*h* posses mixed ionic and covalent type of chemical bonding, the top-most VB is not
46 well dispersive to provide good electrical conductivity by *p*-type doping. So, we focus attention to well
47 dispersive CB minimum and conductivity by electrons. The second band gap $E_g^*$=1.76 eV is sufficient to
48 provide transparency in the near infra red (IR) region of the solar spectra. Such hydrides can find appli-
49 cations as buffer layer, e.g. in structures like TCO/hydride/Si which will replace TCO/a-Si:H/Si. Howev-
50 er, some of the interband transitions in the CB can sometimes be forbidden due to symmetry restrictions.
51



000000 physica (b) 243/z WordXP Art.: W0000/Autor M:\Brage-publikasjoner\Physica-status-solidi-A-Applied-research-.200723171.doc
&R310; insgesamt 11 Seiten 15.09.2017 Bearb.:

1 If such forbidden transitions correspond to visible part of the solar spectra, then transparency of the ma-
2 terial in the visible spectra has a chance for surviving. Also, heavy doping with shallow level defects can
3 enhance not only conductivity but also reflectivity of the material. In order to check whether it destroys
4 transparency we have studied total density of states (DOS) for Si doped $AlH_3$-*h* (Fig. 2). Si atoms substi-
5 tuting Al ($Si_{Al}$) are found to form a band connected to the top-most VB of $AlH_3$-*h*. Consequently, Si
6 doped $AlH_3$-*h* can be good electrical conductor.
7 Figure 3 presents absorption coefficient ($\alpha(\hbar\omega)$) and reflectivity ($R(\hbar\omega)$) for the Si doped $AlH_3$-*h*. It
8 is seen that in $AlH_3$-*h*:$Si_{Al}$ the magnitude of $\alpha(\hbar\omega)$ is considerably small in the visible spectra, but reflec-
9 tivity $R(\hbar\omega)$ is very high at the energy range 0-1 eV. However, at energies 1-4 eV magnitude of $R(\hbar\omega)$ is
10 also within the reasonable limit. Consequently, at low doping levels $<10^{15}$ cm$^{-3}$, the Si doped $AlH_3$-*h* can
11 be transparent to the visible spectra and at the same time will posses *n*-type conductivity.
12 Analysis of band structure for $AlH_3$-*o* (Fig. 4) shows that the calculated fundamental and second
13 band gaps are 2.8 eV and 0.7 eV, respectively. The real fundamental band gap is expected to be larger
14 than the theoretically calculated value of 2.8 eV. The bottom-most CB and top-most VB are well disper-
15 sive, thus indicating tendency for good *n*- and *p*-type electrical conductivity. The VB effective masses
16 have been calculated, which are equal to $1.30m_0$ for $\Gamma\rightarrow S$, $0.67m_0$ for $\Gamma\rightarrow Y$, and $2.96m_0$ for $\Gamma\rightarrow Z$. These
17 results show that the hole conductivity is expected to be anisotropic. The calculated VB effective masses
18 are smaller than those for ZnO where the calculated values from FP-LMTO method are $2.74m_0$ ($\Gamma\|A$)
19 and $0.54m_0$ ($\Gamma\perp A$) [17] and our calculated values are 2.27 ($\Gamma\|A$) and $0.35m_0$ ($\Gamma\perp A$). This shows that the
20 mobility of hole in $AlH_3$-*o* will be much larger than that in ZnO.
21 The feature of small second band gap (0.7 eV) and dispersive CB minimum of $AlH_3$-*o* can be useful
22 for the electronic devices those are transparent to the IR region. The well dispersive feature of the top-
23 most VB and large fundamental band gap can be useful for transparency to the visible spectra and p-type
24 conductivity. So, band structure of $AlH_3$-*o* allows both *n*-type and *p*-type conductivities. The *n*-type/*p*-
25 type conductivity can be achieved upon doping by shallow impurities such as group-IV/-II atoms (e.g.,
26 C, Si, etc.)/(Be, Mg, etc.) substituting Al, or by native defects of $AlH_3$-*o*. Group-II atoms (Be, Mg, etc.)
27 substituting H can also expected to be shallow donors.
28 We have studied total DOS of Ca doped $AlH_3$-*o* (Figure 5). Ca atoms substituting Al ($Ca_{Al}$) are
29 expected to form shallow acceptor level and to be the source for *p*-type conductivity. It is seen in Fig. 5
30 that Ca forms shallow acceptor band as expected. In order to check, whether transparency is changed, we
31 have studied optical spectra for $AlH_3$-*o*. The results are presented in Fig. 6. Analysis of Fig. 6 shows that
32 both absorption and reflectivity spectra are considerably small in the visible spectra indicating sufficient
33 transparency even after heavy doping. Consequently, one can ascribe $AlH_3$-*o* into the class of TC materi-
34 als with *p*-type conductivity. Below we discuss advantages of using hydrides in electronic devices.
35
36 **5 Device applications of hydrides**
37 One can use hydrides as buffer layers in optoelectronic devices, say, solar cells, or light emitting
38 diodes where TCO is currently used on top of the semiconductor. Intermediate oxide layer, band offset,
39 and defect states can be formed in such case, which limits the device performance [18, 19]. To avoid it,
40 an intermediate layer is incorporated in between the TCO and the semiconductors. For example a-Si:H
41 for Si solar cells [20] and CdS or several other buffer layers for $Cu(InGa)Se_2$ cells [21]. If hydrides
42 would be used instead of the TCOs, then no oxide layer is expected to form. Thus the need for incorpora-
43 tion of the buffer layer can be excluded at all. Furthermore, hydrides can also be used as alternative to
44 the commonly used buffer layers. For example, a-Si:H with band gap in the range 1.6-1.8 eV could be
45 replaced by $AlH_3$-*h* or $Al_4H_6$-like hydrides with band gap of 1.76 and ~1.9 eV [22], respectively. One of
46 the advantages of using hydrides over a-Si:H is that the band gap of hydrides can be varied in a wider
47 range by defect engineering. This feature can be useful in device technology.
48 Another exciting application of hydrides is that they can be used for spintronic devices. Hydrogen
49 diffusion from the hydride to the semiconductor is not harmful for device operation, because hydrogen
50 posses the feature to passivate the defects states and it can contribute to conductivity [23]. As is well
51

 copyright line will be provided by the publisher

000000 physica (b) 243/z WordXP Art.: W0000/Autor M:\Brage-publikasjoner\Physica-status-solidi-A-Applied-research-.200723171.doc
&R31; insgesamt 11 Seiten 15.09.2017 Bearb.:

known, in spintronics efficiency of the spin injection into semiconductor is limited by the problem of spin disordering at the interface. If the dilute magnetic semiconductor is replaced by dilute magnetic hydride, then spin injection is expected to be more efficient, because of the absence of the intermediate oxide layer and reduced defects states at the interface.

One problem with hydrides, and specifically $AlH_3$, is that they typically react with air and water. Therefore, in any device applications the hydride would need to be protected from the environment. Here it should be noted that even in the conventional solar cells there is an external layer present to protect it from the environment. Upon using the hydrides as a buffer layer the hydride is commonly incorporated in between TCO and the base materials such as Si, CuInGaSe etc. In such applications the hydride is always protected by TCO layer from the environment, similar to the a-Si:H layer in the heterostructure such as TCO/a-Si:H/Si. Therefore, wide-bandgap hydrides have potential advantages over TCOs and buffer layers in case of multilayer based devices, where properties of interfaces are crucial.

In scientific literature (see, e.g., Ref. [3]) hydrides can be classified into metal hydrides and complex hydrides depending on hydrogen content, operating temperature, and hydrogen absorption/desorption kinetics. From metal hydrides the hydrogen can be removed easily even at temperatures below 100ºC. Such hydrides have relatively low weight percentage of stored hydrogen (1.5 to 2.5 wt.%) and they are opaque. In complex hydrides one can store more hydrogen (up to 20.8 wt.% in $Be(BH_4)_2$) [25], they possess wide band gap, but the hydrogenation/dehydrogenation kinetics is slow, and operating temperature is high. Because of these reasons, the complex hydrides are considered to be less preferable for the hydrogen storage purposes. However, they can find application in the electronic device technology. However, the fast hydrogenation/dehydrogenation kinetics is expected to be harmful because it can cause instability in the device operation. Based on this point of view we suggest that the complex hydrides with slow hydrogenation/dehydrogenation kinetics and high operating temperature can be more appropriate candidates for the electronic device applications.

Recently we have predicted several new complex hydrides for hydrogen storage applications (see, e.g., Ref [3]). Our experience shows that it is possible to have thousands of stable complex hydrides, but, only few percent of these compounds were experimentally explored so far. So the research on complex hydrides is in the beginning stage and it has large potential not only in hydrogen storage or hydride electronics but also for other novel applications.

One of the important points is to determine the doping limit, i.e. the largest possible concentration of the impurities to be incorporated into the hydride for providing n- or p-type conductivity without losing their transparency. This issue shall be discussed in forthcoming articles. It is necessary to note also that for some device applications the high doping level ($>10^{19}$ $cm^{-3}$) and conductivity is not the main issue. It is sufficient to use just the semiconductor properties of hydrides with moderate level of *n/p*-type doping ($\sim10^{15}$ $cm^{-3}$). As it is well known, at low levels of doping electronic properties of the host material will not change noticeably. The important finding is that hydrides exhibit both *n*- and *p*-type conductivity being semiconductors.

### 1.1 Conclusion

We have reported novel applications of hydrides in electronic device technology. Using $AlH_3$–*h* and –*o* as a model system we have shown that hydrides have the potential to replace TCOs, buffer layers, as well as they can be used as spintronic materials. Studies about defect engineering, transparency, and feasibility of the *n*- and *p*-type conductivity of hydrides are the subject for detailed investigations in the near future. Present study suggest that hydrides are expected to have the largest impact on electronic device industry similar to a-Si:H, which opened a new frontier called "Giant Microelectronics" [24]. We anticipate that the present finding can lead to future generation of electronic devices called "hydride electronics".

**Acknowledgements** This work has received financial and supercomputing support from the Research Council of Norway and from the Academy of Sciences of Uzbekistan.

copyright line will be provided by the publisher 

000000 physica (b) 243/z WordXP Art.: W0000/Autor M:\Brage-publikasjoner\Physica-status-solidi-A-Applied-research-.200723171.doc
**&R310;** insgesamt 11 Seiten 15.09.2017 Bearb.:

1
2
3
4
5
6
7
8
9
10
11
12
13
14
15
16
17
18
19
20
21
22
23
24
25
26
27
28
29
30
31
32
33
34
35
36
37
38
39
40
41
42
43
44
45
46
47
48
49
50
51

# References


[1] J. N. Huiberts, R. Griessen, et al., Nature **380** 231-234 (1996).

[2] J. W. J. Kerssemakers, S. J. van der Molen, N. J. Koeman, et al., Nature **406** 489-491 (2000).

[3] P. Vajeeston, in PhD thesis "Theoretical Modelling of Hydrides". Department of Physics, Faculty of Mathematics and Natural Sciences, ISSN 1501-7710, No 390. The University of Oslo, Oslo, p. 390, 2004.

[4] G. Kresse and J. Furthmüller, Phys. Rev. B **54** 11169-11186 (1996).

[5] G. Kresse and J. Hafner, Phys. Rev. B **47** 558-561 (1993).

[6] J. P. Perdew, K. Burke, and M. Ernzerhof, Phys. Rev. Lett. **77** 3865-3868 (1996).

[7] S. Z. Karazhanov, P. Ravindran, A. Kjekshus, et al., Phys. Rev. B **75** 155104 (2007).

[8] M. J. van Setten, V. A. Popa, G. A. de Wijs, et al., Phys. Rev. B **75** 035204 (2007).

[9] X. Z. Ke, A. Kuwabara, and I. Tanaka, Phys. Rev. B **71**(2005).

[10] J. Graetz and J. J. Reilly, J. Alloys Compd **424** 262-265 (2006).

[11] J. Graetz, S. Chaudhuri, et al., Phys. Rev. B **74** 214114 (2006).

[12] S. Orimo, Y. Nakamori, T. Kato, et al., App. Phys. A: Mater. Sci. Proc. **83** 5-8 (2006).

[13] J. Graetz and J. J. Reilly, etc. J. Phys. Chem. B **109** 22181-22185 (2005).

[14] G. Sandrock, J. Reilly, J. Graetz, et al., Appl. Phys. A: Mater. Sci. & Proc. **80** 687-690 (2005).

[15] C. Wolverton, V. Ozolins, and M. Asta, Phys. Rev. B **69**(2004).

[16] J. W. Turley and H. W. Rinn, Inorg. Chem. **8** 18-& (1969).

[17] W. R. L. Lambrecht, A. V. Rodina, S. Limpijumnong, et al., Phys. Rev. B **65** 075207 (2002).

[18] A. G. Ulyashin, R. Job, M. Scherff, et al., Thin Solid Films **403-404** 359-362 (2002).

[19] H. Kobayashi, T. Ishida, Y. Nakato, et al., J. Appl. Phys. **63** 1736-1743 (1991).

[20] M. Taguchi, K. Kawamoto, et al., Progr. Photovolt. **8** 503 (2000).

[21] W. N. Shafarman and L. Stolt, in Handbook of Photovoltaic Science and Engineering (A. LUQUE and S. HEGEDUS, eds.), Lohn Wiley & Sons, LTD., 2003.

[22] X. Li, A. Grubisic, S. T. Stokes, et al., Science **315** 356-358 (2007).

[23] C. G. Van de Walle and J. Neugebauer, Nature **423** 626-628 (2003).

[24] P. G. Lecomber and W. E. Spear, Phys. Rev. Lett. **25** 509-511 (1970).

[25] L. Schlapbach and A. Züttel, Nature **414**, 353 (2001).



copyright line will be provided by the publisher

000000 physica (b) 243/z WordXP Art.: W0000/Autor M:\Brage-publikasjoner\Physica-status-solidi-A-Applied-research-.200723171.doc
&R31; insgesamt 11 Seiten 15.09.2017 Bearb.:

1
2
3
4
5
6
7
8
9
10
11
12
13
14
15
16
17
18
19
20
21
22
23
24
25
26
27
28
29
30
31
32
33
34
35
36
37
38
39
40
41
42
43
44
45
46
47
48
49
50
51

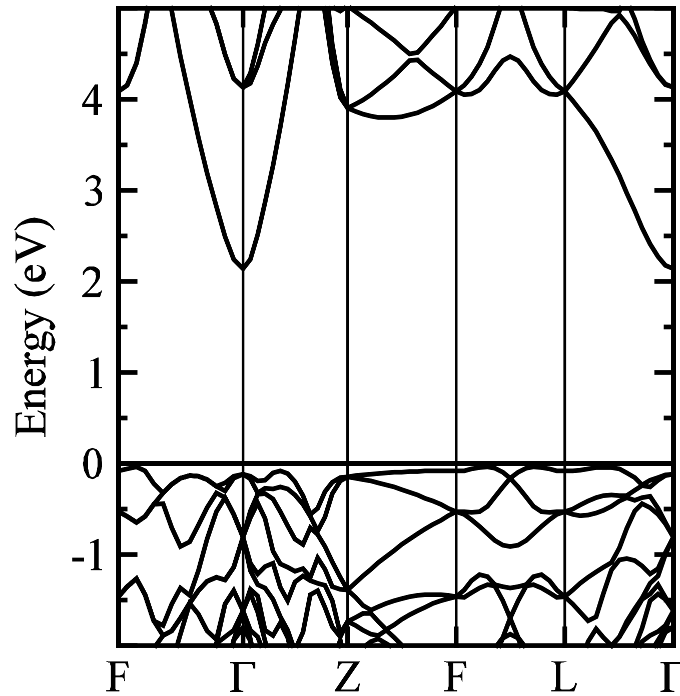


Fig. 1. Band dispersion for $AlH_3$-*h*. Fermi level is set to zero.

copyright line will be provided by the publisher



000000 physica (b) 243/z WordXP Art.: W0000/Autor M:\Brage-publikasjoner\Physica-status-solidi-A-Applied-research-.200723171.doc
**&R310;** insgesamt 11 Seiten 15.09.2017 Bearb.:

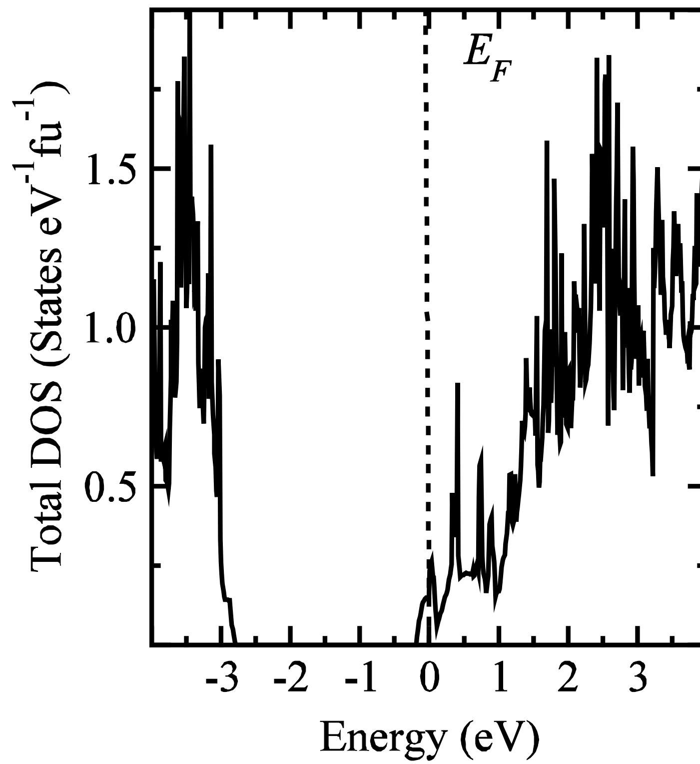


Fig. 2. Total DOS for $AlH_3$-*h* doped with $Si_{Al}$. Fermi level is set to zero.

 copyright line will be provided by the publisher

000000 physica (b) 243/z WordXP Art.: W0000/Autor M:\Brage-publikasjoner\Physica-status-solidi-A-Applied-research-.200723171.doc
&R31; insgesamt 11 Seiten 15.09.2017 Bearb.:

1
2
3
4
5
6
7
8
9
10
11
12
13
14
15
16
17
18
19
20
21
22
23
24
25
26
27
28
29
30
31
32
33
34
35
36
37
38
39

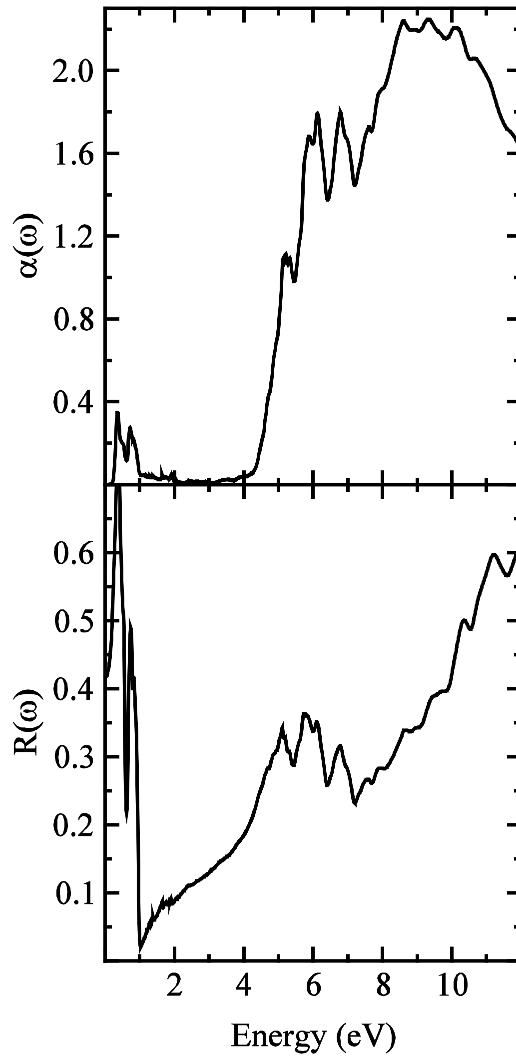


40 Fig. 3 Absorption coefficient α(ω) and reflectivity R(ω) for Si doped $AlH_3$-*h*. α(ω) is given in $cm^{-1}$ divided by $10^5$.

41 21
42 22
43 23
44 24
45 25
46 26
47 27
48 28
49 29
50 30
51 31

1 32
2 33
3 34
4 35
5 36
6 37
7 38
8 39

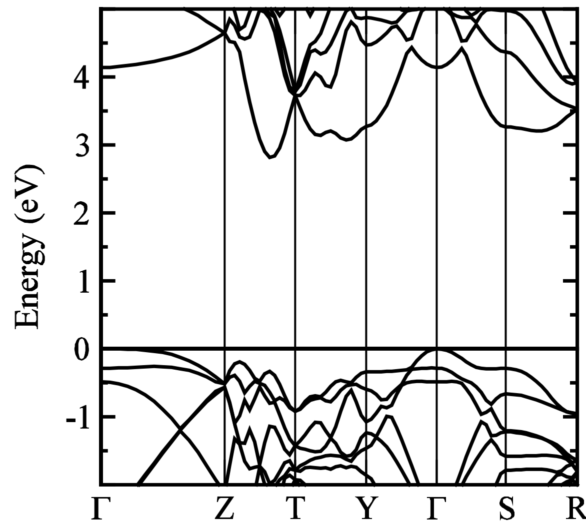


Fig. 4. Band dispersion for $AlH_3$-*o*. Fermi level is set to zero.

40
41

1
2
3
4
5
6
7
8
9
10
11
12
13
14
15
16
17
18
19
20
21
22
23
24
25
26
27
28
29
30
31
32
33
34
35
36
37
38
39
40
41
42
43
44
45
46
47
48
49
50
51

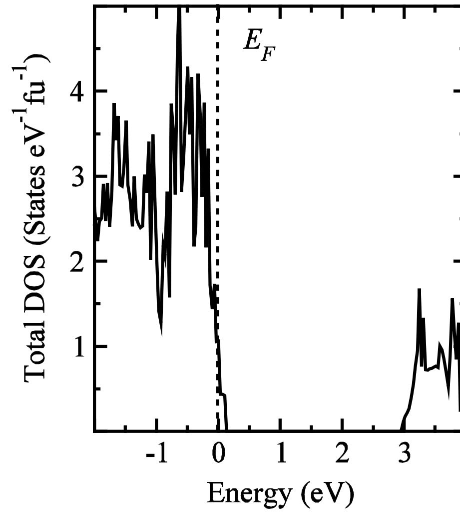


Fig. 5. Total DOS for $AlH_3$-*o* with $Ca_{Al}$.

42
43
44

Fig. 6. Absorption coefficient α(ω), and reflectivity R(ω) for $AlH_3$-*o* with $Ca_{Al}$. α(ω) is given in $cm^{-1}$ divided by $10^5$.

45
46
47
48
49
50
51gggggggggggggggggggggggggggggggggggggggggggggggggggggggggggggggggggggggg

 copyright line will be provided by the publisher

000000 physica (b) 243/z WordXP Art.: W0000/Autor M:\Brage-publikasjoner\Physica-status-solidi-A-Applied-research-.200723171.doc
&R31; insgesamt 11 Seiten 15.09.2017 Bearb.: